2009

On the phase diagram of water with density functional theory potentials: The melting temperature of ice /h with the Perdew–Burke–Ernzerhof and Becke–Lee–Yang–Parr functionals

Soohaeng Yoo
Pacific Northwest National Laboratory

Xiao Cheng Zeng
University of Nebraska-Lincoln, xzeng1@unl.edu

Sotiris C. Xantheas
Pacific Northwest National Laboratory

On the phase diagram of water with density functional theory potentials: The melting temperature of ice I_h with the Perdew–Burke–Ernzerhof and Becke–Lee–Yang–Parr functionals

Soohaeng Yoo,[1] Xiao Cheng Zeng,[2,a)] and Sotiris S. Xantheas[1,a)]
[1]*Chemical and Materials Sciences Division, Pacific Northwest National Laboratory, 902 Battelle Boulevard, MS K1-83, Richland, Washington 99352, USA*
[2]*Department of Chemistry, University of Nebraska-Lincoln, Lincoln, Nebraska 68588, USA*

(Received 17 February 2009; accepted 22 May 2009; published online 11 June 2009)

The melting temperature (T_m) of ice I_h was determined from constant enthalpy and pressure (*NPH*) Born–Oppenheimer molecular dynamics simulations to be 417 ± 3 K for the Perdew–Burke–Ernzerhof and 411 ± 4 K for the Becke–Lee–Yang–Parr density functionals using a coexisting ice (I_h)-liquid phase at constant pressures of $P=2500$ and 10 000 bar and a density $\rho=1$ g/cm^3, respectively. This suggests that ambient condition simulations at $\rho=1$ g/cm^3 will rather describe a supercooled state that is overstructured when compared to liquid water. © *2009 American Institute of Physics*. [DOI: 10.1063/1.3153871]

Water remains an active field of research in the quest to obtain a quantitative description of its properties over a wide range of temperatures and pressures.[1–3] In the biological and chemical fields, water plays a pivotal role in the stabilization of biomolecules[4,5] and the acid-base chemical reactions.[6–8] A molecular level account of water has been sought for almost a century relying on both classical and quantum descriptions of the underlying intermolecular interactions. The latter offer the flexibility of being able to describe the chemical[6–12] and physical[13–21] properties of water through electronic structure calculations and for this reason have become increasingly popular with the advent of powerful supercomputers.

There have been several previous efforts to obtain structural information for water at ambient conditions, viz. the radial distribution function (RDF) and structure factors, from density functional theory (DFT)-based molecular dynamics simulations[14–21] and compare them with the experimentally available data.[22,23] Based on the comparison of the computed RDFs with experiment, it has been previously inferred that DFT yields in general an overstructured liquid at $\rho=1$ g/cm^3 and ambient conditions.[16–18] This naturally raises the question of what is the phase diagram of water predicted by the various DFT functionals and whether DFT simulations at ambient conditions will also produce a supercooled liquid, given the fact that water, like other "tetrahedral liquids,"[24,25] is also more structured at the metastable supercooled phase.[2,26,27] To address those issues one needs to know the melting temperature (T_m) of water described by DFT functionals, a starting point in obtaining its phase diagram with a DFT-based simulation. Although T_m for water under high pressure (10–50 GPa) has been previously reported[28] with a DFT-based simulation, the one under ambient conditions is not yet known. In this study we report the melting temperature of water with the Perdew–Burke–Ernzerhof (PBE)[29] and Becke–Lee–Yang–Parr (BLYP)[30,31] functionals using Born–Oppenheimer molecular dynamics (BOMD) simulations.

Two main approaches have traditionally been used to estimate the melting temperature via computer simulations: one is based on the direct simulation of the solid-liquid coexistence[32–37] while the other is based on the thermodynamic integration of the free energy of the solid and liquid phases. In the second approach T_m is determined by the condition of equality of the Gibbs free energies of the liquid and solid,[38] viz. $G_{\mathrm{liq}}(P,T)_{T=T_m}=G_{\mathrm{solid}}(P,T)_{T=T_m}$. Previous DFT-based simulations have reported T_m using a coexisting solid-liquid phase for metals [Al,[39] Fe,[40] Ta (Ref. 41)], MgO,[42] and also water under high pressure[28] but, as stated earlier, there is currently no information about the T_m of water under ambient conditions from a DFT-based simulation.

For the calculation of T_m we adopted the (*NPH*) ensemble, i.e., constant pressure (P), particle number (N), and enthalpy (H), of the coexisting ice-liquid phase.[35] MD simulations in the (*NPH*) ensemble with the ice-liquid coexistence phase allows for the temperature to be adjusted spontaneously into the condition that satisfies $G_{\mathrm{liq}}(P,T)=G_{\mathrm{solid}}(P,T)$. The (*NPH*) ensemble is preferable [relative to the (*NVE*) ensemble] in calculating the point (P, T_m) at a given pressure on the phase diagram. Another advantage lies in that the stress-anisotropy problem is never an issue since the three principle components of the stress tensor can be adjusted to the given pressure. In preparing the simulation system, an initial configuration of the proton-disordered ice was constructed in order to meet the conditions such that the Bernal–Fowler rules are satisfied and that the cell has a zero total dipole moment.[43] The ice-liquid coexisting system consists of 192 water molecules (initially 96 icelike and 96 liquidlike) in a simulation cell of dimensions $13\times15\times28$ Å^3 (see Fig. 1). The initial configuration for the BOMD (*NPH*) simulations was constructed as follows: we obtained the liquid phase from classical MD simulations with the TIP4P

a)Authors to whom correspondence should be addressed. Electronic addresses: sotiris.xantheas@pnl.gov and xczeng@phase2.unl.edu.

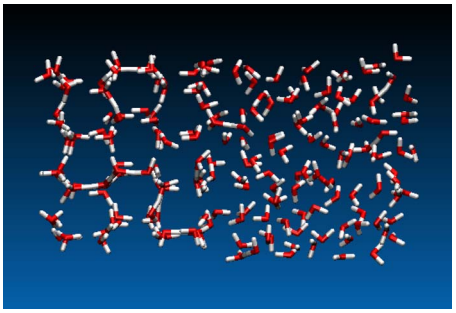

FIG. 1. (Color online) A snapshot of the coexisting ice-liquid simulation with the PBE functional in the (*NPH*) ensemble at $P=2500$ bar and $T=450$ K.

model[44] after an equilibration period of 100 ps at 300 K, we then merged it with the ice phase and performed a short (5 ps) BOMD (*NPT*) simulation for this coexisting system. Our choice regarding the size of the simulation cell—mainly dictated by the cost of the BOMD simulations—raises an issue regarding system size effects and convergence of the results. Previous studies[35] with the TIP4P classical interaction potential used a simulation cell of 12 288 molecules and produced—under the same simulation protocol—a melting temperature of $T=229\pm1$ K. When a smaller simulation cell of 192 molecules (similar to the one employed in this study) is used with the same (TIP4P) potential, the melting temperature is lowered to ~200 K. Thus, assuming that the qualitative behavior between TIP4P and PBE/BLYP as regards to the variation in the melting temperature with simulation cell size is the same, the melting temperatures for the two functionals reported in this study can be probably considered as a lower limit.

The calculations were performed using QUICKSTEP,[45] which is part of the CP2K program package, ported in the "Chinook" supercomputer at Pacific Northwest National Laboratory (PNNL). The required wall-time for 1 ps BOMD simulation is typically 10 h using 160 CPUs of the Chinook supercomputer at PNNL. Water was described at the DFT level with the hybrid Gaussian and plane-wave method. The core electrons were removed by the introduction of norm-conserving pseudopotentials developed by Goedecker and coworkers[46,47] and the charge density cutoff of 280 Ry was used for the auxiliary basis set. The PBE (Ref. 29) and BLYP[30,31] exchange-correlation functionals were used. Kohn–Sham orbitals were expanded into a double-ζ valence basis (denoted as DZVP) for the PBE functional, while a triple-zeta valence basis set augmented with two sets of *d*-type or *p*-type polarization functions (TZV2P) was used for the BLYP functional. During the BOMD simulations the electronic structure is recomputed at every time step by iterative minimization. The nuclear equation of motion was integrated using a standard velocity Verlet algorithm with a 0.5 fs time step and hydrogen masses. We used a strict convergence criterion of the wave function (convergence criterion for the electronic gradient $\varepsilon_{\mathrm{SCF}}\leq 1\times10^{-7}$ with the orbital transformation method).

Without *a priori* information on the phase diagram of water with the PBE and BLYP functionals, we first obtained the corresponding average pressure at $\rho=1$ g/cm^3. For this

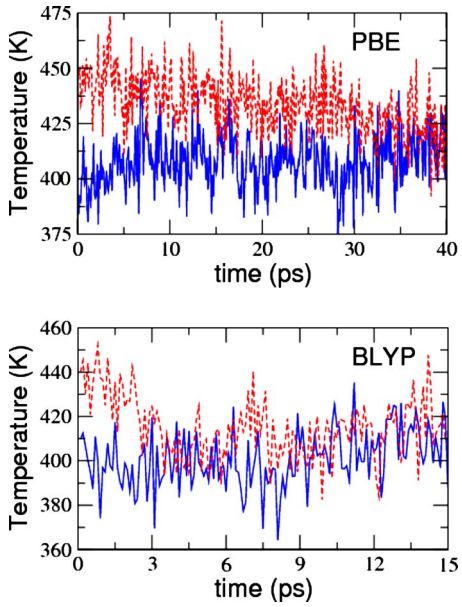

FIG. 2. (Color online) The coexisting ice-liquid simulation in the (*NPH*) ensemble with the PBE (top) and BLYP (bottom) functionals. Two initial systems are prepared using (*NPT*) BOMD simulations (~5 ps) at $T=400$ K (solid line in blue) and $T=450$ K (dashed line in red), respectively.

purpose, the TIP4P snapshots were used to obtain average pressures of $P=2500$ bar (PBE) and $P=10\,000$ bar (BLYP). Subsequently, three independent simulations were run at different initial temperatures, viz. $T=350$, 400, and 450 K. The evolution of the instantaneous kinetic temperature was monitored for ~40 ps (PBE) and ~15 ps (BLYP). Figure 2 shows the results of the instantaneous kinetic temperature T versus the simulation time t for the two initial temperatures of $T=400$ and 450 K. The kinetic temperatures of the two systems gradually converge to the values of T_m $\sim417\pm3$ K (PBE) and $\sim411\pm4$ K (BLYP), respectively. As it can be seen from Fig. 2, convergence is achieved in the first 35 ps (PBE) and 10 ps (BLYP) and the next 5 ps were used for the estimation of the error bars based on the standard deviation. Schwegler *et al.*[17] have previously suggested that a temperature of ~415 K with the PBE functional is necessary to obtain values for the diffusion coefficient that are comparable to experiment at ambient conditions for BOMD (classical) simulations. Their suggestion was based solely on the comparison between the calculated oxygen-oxygen RDFs and diffusion coefficient and their experimental values. In contrast, our study provides T_m based on the thermodynamic criterion that the free energy of ice is equal to that of the liquid at the melting temperature. The previous estimate by Schwegler *et al.*,[17] as well as the current study, do not include nuclear quantization,[6,48–51] an effect that has been reported to increase the diffusion coefficient by a factor of as much as 1.6 times with respect to the classical result.[48,49] Previous studies have further suggested that quantum effects induce structural and dynamical changes in the order of 30–50 K, that is, the quantum system is described by the classical system at elevated temperatures at constant density.[17,51] In particular, Kuharski and Rossky[51] have arrived at an estimate of 50 K using the rigid ST2 potential, whereas recently Paesani *et al.*[49] suggested a value of

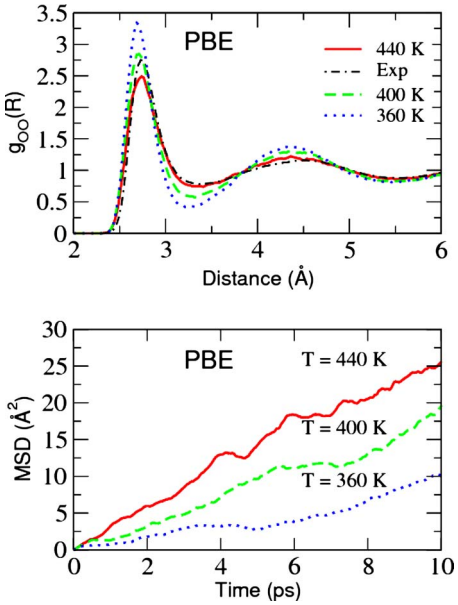

FIG. 3. (Color online) The oxygen-oxygen RDFs (top) and the MSDs (bottom) from (*NVT*) simulations of a supercell of 125 water molecules at $\rho=1$ g/cm^3 with the PBE functional at $T=440$, 400, and 360 K, respectively. The dashed line corresponds to the experimental oxygen-oxygen RDF.

25–30 K for this effect based on simulations with the flexible, polarizable TTM2.1-F potential.[52] They also showed that this is not a unique temperature factor since quantum effects vary in a nonlinear fashion as a function of the temperature. Assuming a 30 K effect as proposed by Paesani *et al.*[49] (albeit with the TTM2.1-F classical flexible, polarizable potential) the estimated melting temperature is lowered to ~387 K (PBE) and ~381 K (BLYP). Although this shift is in the right direction, it still produces an estimate for the melting temperature that is over 100 K larger than the experimental value.

In order to further investigate the effect of temperature on the structure of water with the PBE functional, we performed additional independent (*NVT*) simulations at three different temperatures $T=360$, 400, and 440 K using supercells consisting of 125 water molecules at $\rho=1$ g/cm^3. After equilibrating the system for 10 ps, the statistics were collected for another 10 ps. The average pressure of PBE water at $\rho=1$ g/cm^3 and $T=440$ K is 3000 bar, which is very close to the average pressure obtained using the TIP4P snapshots. Figure 3(a) shows the oxygen-oxygen RDF, $g_{OO}(R)$, for the three different temperatures considered here. The change in the shape of the curves clearly reflects the strong effect of temperature on the structure of water. The height of the first maximum of $g_{OO}(R)$ at $T=440$ K is 2.5, lower than the experimental value[23] of 2.8. However, for $R_{OO}>3$ Å (the region that includes the second coordination shell) it shows a good agreement with experiment, suggesting that the PBE functional produces a stable liquid phase at this temperature. In contrast, for $T=400$ K the region of the first peak in $g_{OO}(R)$ is also consistent with experiment, but the part of the $g_{OO}(R)$ beyond 3 Å appears more structured. Finally the RDF at $T=360$ K represents a typical example of a supercooled liquid. The average coordination numbers (CNs) are 4.6, 4.4, and 4.0 at $T=440$, 400, and 360 K, respectively. Note that the CN at $T=440$ K is in very good agreement with the experimental value[23] of 4.7. The supercooled liquid at $T=360$ K preserves much of its icelike tetrahedral structure.

The mean square displacement (MSD) curves for the three temperatures are shown in Fig. 3(b). They are related to the diffusion constant (D) according to

$$D=\frac{\mathrm{MSD}}{6t}=\lim_{t\to\infty}\frac{1}{6t}\left\langle\frac{1}{N}\sum_i|\mathbf{r}_i(t)-\mathbf{r}_i(0)|^2\right\rangle.$$

The MSDs were computed from the relative displacements of the oxygen atoms and averaged over all water molecules and all configurations of the full trajectory.[38] The calculated diffusion coefficients are 0.425 Å^2/ps ($T=440$ K), 0.327 Å^2/ps ($T=400$ K), and 0.169 Å^2/ps ($T=360$ K). Assuming a uniform 60% increase[48,49] due to quantum effects, we obtain "quantum-corrected" values for the diffusion coefficients of 0.68 Å^2/ps ($T=440$ K), 0.523 Å^2/ps ($T=400$ K), and 0.270 Å^2/ps ($T=360$ K). For comparison, the experimental value is 0.24 Å^2/ps at ambient conditions. This supports the proposition of a "liquidlike" behavior at $T=440$ K and it is consistent with the estimate of $T_m=417\pm3$ K.

In summary, we calculated the melting temperature of water with the PBE and BLYP density functionals using a coexisting ice (I_h)-liquid system. Our estimates are $T_m=417\pm3$ K at $P=2500$ bar (PBE) and $T_m=411\pm4$ K at $P=10\,000$ bar (BLYP). System size effects suggest that this value is probably a lower limit for the melting temperature, whereas the inclusion of nuclear quantum effects produces estimates that are >100 K larger than the experimental value. Based on this finding, the calculated oxygen-oxygen RDFs and MSDs for $\rho=1$ g/cm^3 at $T=360$, 400, and 440 K furthermore suggested that the liquid phase is supercooled below the melting temperature. These results can therefore explain why the PBE and BLYP functionals produce an overstructured liquid at room temperature and up to 400 K. In order to study the physical, thermodynamic, and structural properties of water with these two functionals and compare with experiment at ambient conditions, simulations at $T>T_m$ need to be performed. Since T_m is probably sensitive to different DFT functionals, it is expected that the phase diagram (including T_m) of water with other popular hybrid and/or meta-DFT functionals [such as B3LYP,[30,31,53] TPSS,[54] and M06–2X (Ref. 55)] could be different from the current results obtained with the PBE and BLYP functionals. Thus, special care should be exercised when choosing the temperature of a simulation for the liquid phase of water using DFT functionals, to ensure that a liquid rather than a supercooled phase is simulated.

This work was supported by the Chemical Sciences, Geosciences, and Biosciences Division and the Materials Science and Engineering Division (DE-FG02-04ER46164), Office of Basic Energy Sciences, U.S. Department of Energy, and by the Nebraska Research Initiative. Battelle operates the Pacific Northwest National Laboratory for the U.S. Department of Energy. This research was performed in part using the Molecular Science Computing Facility (MSCF) in

the Environmental Molecular Sciences Laboratory, a national scientific user facility sponsored by the Department of Energy's Office of Biological and Environmental Research. Additional computer resources were provided by the Office of Basic Energy Sciences, U.S. Department of Energy.

[1] P. H. Poole, F. Sciortino, U. Essmann, and H. E. Stanley, Nature (London) **360**, 324 (1992).
[2] C. A. Angell, Science **319**, 582 (2008).
[3] P. Ball, Nature (London) **452**, 291 (2008).
[4] M. Chaplin, Nat. Rev. Mol. Cell Biol. **7**, 861 (2006).
[5] P. Ball, Chem. Rev. (Washington, D.C.) **108**, 74 (2008).
[6] M. E. Tuckerman, D. Marx, M. L. Klein, and M. Parrinello, Science **275**, 817 (1997).
[7] D. Marx, M. E. Tuckerman, J. Hutter, and M. Parrinello, Nature (London) **397**, 601 (1999).
[8] P. L. Geissler, C. Dellago, D. Chandler, J. Hutter, and M. Parrinello, Science **291**, 2121 (2001).
[9] M. E. Tuckerman, D. Marx, and M. Parrinello, Nature (London) **417**, 925 (2002).
[10] H. J. Bakker and H. K. Nienhuys, Science **297**, 587 (2002).
[11] M. Rini, B. Z. Magnes, E. Pines, and E. T. Nibbering, Science **301**, 349 (2003).
[12] O. F. Mohammed, D. Pines, J. Dreyer, E. Pines, and E. T. Nibbering, Science **310**, 83 (2005).
[13] D. Asthagiri, L. R. Pratt, and J. D. Kress, Phys. Rev. E **68**, 041505 (2003).
[14] K. Laasonen, M. Sprik, and M. Parrinello, J. Chem. Phys. **99**, 9080 (1993).
[15] M. Sprik, J. Hutter, and M. Parrinello, J. Chem. Phys. **105**, 1142 (1996).
[16] J. C. Grossman, E. Schwegler, E. W. Draeger, F. Gygi, and G. Galli, J. Chem. Phys. **120**, 300 (2004).
[17] E. Schwegler, J. C. Grossman, F. Gygi, and G. Galli, J. Chem. Phys. **121**, 5400 (2004).
[18] M. J. McGrath, J. I. Siepmann, I. F. W. Kuo, C. J. Mundy, J. VandeVondele, F. Mohamed, and M. Krack, ChemPhysChem **6**, 1894 (2005).
[19] J. VandeVondele, F. Mohamed, M. Krack, J. Hutter, M. Sprik, and M. Parrinello, J. Chem. Phys. **122**, 014515 (2005).
[20] M. J. McGrath, J. I. Siepmann, I. F. W. Kuo, C. J. Mundy, J. VandeVondele, J. Hutter, F. Mohamed, and M. Krack, J. Phys. Chem. A **110**, 640 (2006).
[21] K. Leung and S. B. Rempe, Phys. Chem. Chem. Phys. **8**, 2153 (2006).
[22] G. Hura, J. M. Sorenson, R. M. Glaeser, and T. Head-Gordon, J. Chem. Phys. **113**, 9140 (2000).
[23] J. M. Sorenson, G. Hura, R. M. Glaeser, and T. Head-Gordon, J. Chem. Phys. **113**, 9149 (2000).
[24] S. Sastry and A. C. Angell, Nature Mater. **2**, 739 (2003).
[25] Y. Katayama, T. Mizutani, W. Utsumi, O. Shimomura, M. Yamakata, and K. Funakoshi, Nature (London) **403**, 170 (2000).
[26] O. Mishima and H. E. Stanley, Nature (London) **396**, 329 (1998).
[27] I. Brovchenko, A. Geiger, and A. Oleinikova, J. Chem. Phys. **123**, 044515 (2005).
[28] E. Schwegler, M. Sharma, F. Gygi, and G. Galli, Proc. Natl. Acad. Sci. U.S.A. **105**, 14779 (2008).
[29] J. P. Perdew, K. Burke, and M. Ernzerhof, Phys. Rev. Lett. **77**, 3865 (1996).
[30] A. D. Becke, Phys. Rev. A **38**, 3098 (1988).
[31] C. Lee, W. Yang, and R. G. Parr, Phys. Rev. B **37**, 785 (1988).
[32] U. Landman, W. D. Luedtke, R. N. Barnett, C. L. Cleveland, M. W. Ribarsky, E. Arnold, S. Ramesh, H. Baumgart, A. Martinez, and B. Khan, Phys. Rev. Lett. **56**, 155 (1986).
[33] J. R. Morris, C. Z. Wang, K. M. Ho, and C. T. Chan, Phys. Rev. B **49**, 3109 (1994).
[34] S. Yoo, X. C. Zeng, and J. R. Morris, J. Chem. Phys. **120**, 1654 (2004).
[35] J. Wang, S. Yoo, J. Bai, J. R. Morris, and X. C. Zeng, J. Chem. Phys. **123**, 036101 (2005).
[36] R. García Fernández, J. L. Abascal, and C. Vega, J. Chem. Phys. **124**, 144506 (2006).
[37] J. L. Abascal, R. G. Fernández, C. Vega, and M. A. Carignano, J. Chem. Phys. **125**, 166101 (2006).
[38] D. Frenkel and B. Smit, *Understanding Molecular Simulation From Algorithms to Applications* (Academic, San Diego, 2001).
[39] D. Alfè, Phys. Rev. B **68**, 064423 (2003).
[40] D. Alfè, Phys. Rev. B **79**, 060101 (2009).
[41] S. Taioli, C. Cazorla, M. J. Gillan, and D. Alfè, Phys. Rev. B **75**, 214103 (2007).
[42] D. Alfè, Phys. Rev. Lett. **94**, 235701 (2005).
[43] J. A. Hayward and J. R. Reimers, J. Chem. Phys. **106**, 1518 (1997).
[44] W. L. Jorgensen, J. Chandrasekhar, J. D. Madura, R. W. Impey, and M. L. Klein, J. Chem. Phys. **79**, 926 (1983).
[45] J. VandeVondele, M. Krack, F. Mohamed, M. Parrinello, T. Chassaing, and J. Hutter, Comput. Phys. Commun. **167**, 103 (2005).
[46] S. Goedecker, M. Teter, and J. Hutter, Phys. Rev. B **54**, 1703 (1996).
[47] C. Hartwigsen, S. Goedecker, and J. Hutter, Phys. Rev. B **58**, 3641 (1998).
[48] J. A. Poulsen, G. Nyman, and P. J. Rossky, Proc. Natl. Acad. Sci. U.S.A. **102**, 6709 (2005).
[49] F. Paesani, S. Iuchi, and G. A. Voth, J. Chem. Phys. **127**, 074506 (2007).
[50] G. S. Fanourgakis, G. K. Schenter, and S. S. Xantheas, J. Chem. Phys. **125**, 141102 (2006).
[51] R. A. Kuharski and P. J. Rossky, J. Chem. Phys. **82**, 5164 (1985).
[52] G. S. Fanourgakis and S. S. Xantheas, J. Phys. Chem. A **110**, 4100 (2006); C. J. Burnham and S. S. Xantheas, J. Chem. Phys. **116**, 5115 (2002).
[53] A. D. Becke, J. Chem. Phys. **98**, 5648 (1993).
[54] J. Tao, J. P. Perdew, V. N. Staroverov, and G. E. Scuseria, Phys. Rev. Lett. **91**, 146401 (2003).
[55] Y. Zhao and D. G. Truhlar, Theor. Chem. Acc. **120**, 215 (2008).